

News about Bhabha Scattering

Janusz Gluza, Katowice

based on work with:

S. Actis, (Aachen), T. Riemann (DESY),

M. Czakon (U. Würzburg)

Heptools first annual meeting, Athens 2007

- **Introduction: Two-Loop corrections to Bhabha Scattering**
- **The Heavy Fermion Contributions**
 1. $m_e^2 \ll m_f^2 \ll s, t$ [**Nucl.Phys.B786:26-51,2007**]
 2. $m_e^2 \ll m_f^2, s, t$ [**Ustron proceedings, arXiv:0710.5111**]
- **Hadronic contributions [hep-ph/today \[should be!\]](#)**
- **Summary**

The Physics Needs

ILC – Need Bhabha cross-sections with **3–4 significant digits**.

Why?

- **ILC**: $e^+e^- \rightarrow W^+W^-, f\bar{f}$ with $O(10^6)$ events $\rightarrow 10^{-3}$
- **GigaZ**: relevant physics derived from $Z \rightarrow \text{hadrons}, l^+l^-$, the latter with $O(10^8)$ events $\rightarrow 10^{-4}$
- **Low energies (meson factories)**: similar accuracy is needed

The aim:

$$\Delta \mathcal{L}/\mathcal{L} \approx 2 \times 10^{-4} [0.02\%] \text{ for GiGaZ (and } 10^{-3} \text{ for other machines)}$$

Some numbers

A cross-section prediction with **5 significant digits**.

Perturbative orders:

$$\left(\frac{\alpha}{\pi}\right) = 2 \times 10^{-3}$$

$$\left(\frac{\alpha}{\pi}\right)^2 = 0.6 \times 10^{-5}$$

Kinematics:

$$T = -t = 4(E^2 - m_e^2) \sin^2 \Theta / 2$$

$$E = 1 GeV$$

$$m_e^2 \ll T, \text{ e.g.: } 2.61119896 \cdot 10^{-7} \ll 0.00274092978 \text{ (3°), } 1.99999948 \text{ (90°)}$$

$$m_\mu^2 ? T, \text{ e.g.: } 0.0111636909 > 0.00274092978 \text{ (3°)}$$

- **t -channel exchange dominates everywhere even at very large scattering angles except LAS at narrow peak regions ($\Phi, J/\Psi, Z, \dots$)**
- $m_e^2/s < m_e^2/T \leq 10^{-5} \dots 10^{-7}$, see **Bonciani, Feroglia, hep-ph/0507047**

Status by end of 2004

Established: 10^{-3} MC programs for LEP, ILC

- **BHLUMI v.4.04:** Jadach, Placzek, Richter-Was, Was: CPC 1997
- see also: Jadach, Melles, Ward, Yost: PLB 1996, thesis Melles 1996
- **NLLBHA:** Arbuzov, Fadin, Kuraev, Lipatov, Merenkov, Trentadue: NPB 1997, CERN 96-01
- **SAMBHA:** Arbuzov, Haidt, Matteuzzi, Paganoni, Trentadue: hep-ph/0402211

However,

the nonlogarithmic $O(\alpha^2)$ terms, originating from pure QED radiative 1-loop and from 2-loop diagrams not completely covered

2004, end of LEP era

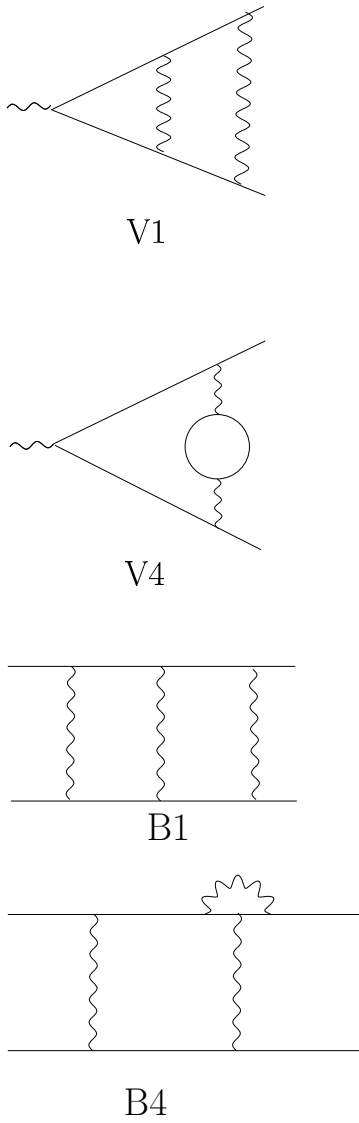
From S. Jadach, hep-ph:0306083

Type of correction/error	LEPEWWG	hep-ph:9811245	hep-ph:9905235	update
Technical precision	—	— (0.03%)	— (0.03%)	0.03%
Missing photonic $\mathcal{O}(\alpha^2 L)$	0.10%	0.027% (0.013%)	0.027% (0.013%)	0.013%
Missing photonic $\mathcal{O}(\alpha^3 L^3)$	0.015%	0.015% (0.006%)	0.015% (0.006%)	0.006%
Vacuum polarization	0.04%	0.04%	0.040%	0.025%
Light pairs	0.03%	0.03%	0.010%	0.010%
Z-exchange	0.015%	0.015%	0.015%	0.015%
Total	0.11%	0.061% (0.062%)	0.054% (0.055%)	0.045%

Virtual 2-loop corrections to Bhabha scattering - recent progress

- 2004, Bonciani, R. and Ferroglia, A. and Mastrolia, P. and Remiddi, E. and van der Bij, J, $N_f = 1$: SE, vertices and a box
- 2005, Czakon, JG, Riemann, Master integrals identified
- 2005, Penin, Non-logarithmic photonic corrections
- 2006, Czakon, JG, Riemann, All massive, planar $n_f = 1$ boxes solved in the limit $m_e^2 \ll s, t, u$
- 2007, Becher, Melnikov; Czakon, JG, Riemann $N_f = 2$, $m_e^2 \ll m_f^2 \ll s, t, u$ + independent confirmation of $N_f = 1$ and photonic calculations
- 2007, Bonciani, Feroglia, Penin; Czakon, JG, Riemann, $N_f = 2$, $m_e^2 \ll m_f^2, s, t, u$ (so can be also used for low energy physics)
- New: Czakon, JG, Riemann, hadronic contributions

Photonic and fermionic $N_f = 1, 2$ topologies



SE loop insertions (without photonic line) are so called **fermionic** diagrams, rest represents **photonic**. Closed fermionic loop can be muon, tau, top or light quarks. Box **B5** is a 3-scale problem: $m_e, m_f, s(t, u)$.

From Guido Montagna's talk, Ustron 2007

Generator	Processes	Theory	Accuracy
Bagenf	e^+e^-	$\mathcal{O}(\alpha)$	0.5%
BabaYaga v3.5	e^+e^- , $\gamma\gamma$, $\mu^+\mu^-$	Parton Shower	0.5 ÷ 1%
BabaYaga@NLO	e^+e^- , $\gamma\gamma$, $\mu^+\mu^-$	$\mathcal{O}(\alpha) + \text{PS}$	~ 0.1%
MCGPJ	e^+e^- , $\mu^+\mu^-$...	$\mathcal{O}(\alpha) + \text{SF}$	< 0.2%
BHWIDE	e^+e^-	$\mathcal{O}(\alpha) \text{ YFS}$	~ 0.5% (_{LEP1})

Table 1: Status of MC generators for luminosity monitoring at meson factories.

Recent 2-loop effects included (photonic and fermionic, $N_f = 1$):

- NNLO QED calculations are important to establish the theoretical accuracy of existing generators and, if necessary, to improve it below 0.1% → so we are calculating heavy fermion and hadronic effects

Determination of master integrals from 2-loop Bhabha scattering

[A] All planar box masters for $m_e^2 \ll s, t, u$

[B] All masters for $N_f = 2$ and $m_e^2 \ll m_f^2 \ll s, t, u$

We had developed for this

Technique of semi-automatized derivation of Mellin-Barnes integrals (→ AMBRE package, 2007)

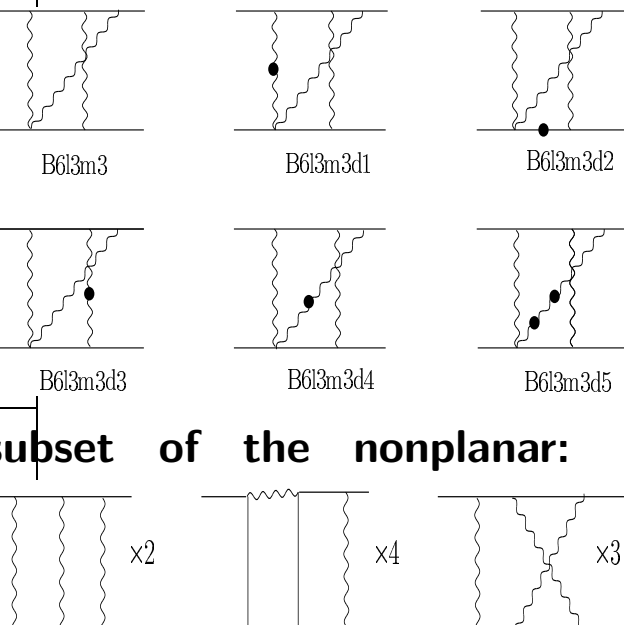
Automatized small-mass expansion for Mellin-Barnes integrals (nontrivial, some integrals must be expanded even to subleading powers to obtain leading power cross section)

We – and all the others – failed with a determination of non-planar 2-loop boxes.
Little is known due to Smirnov, Heinrich.

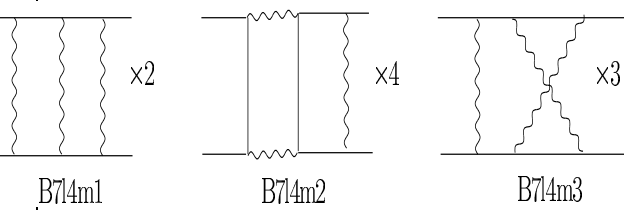
Analytic, expanded

MI	B1	B2	B3	B4	B5	B6	solved:
B714m1	+	-	-	-	-	-	Smirnov:2001, our:2006
B714m1N	+	-	-	-	-	-	Smirnov, Heinrich:2004, our:2006
B714m2	-	+	-	-	-	-	Smirnov, Heinrich:2004 [†] , our:2006
B714m2[d1--d3]	-	+	-	-	-	-	our:2006
B714m3	-	-	+	-	-	-	NP:Smirnov, Heinrich:2004 [†]
B714m3[d1--d2]	-	-	+	-	-	-	NP
B613m1	+	-	+	-	-	-	our:2006
B613m1d	+	-	+	-	-	-	our:2006
B613m2	-	+	-	+	-	-	our:2006
B613m2d	-	+	-	+	-	-	our:2006
B613m3	-	-	+	-	-	-	NP
B613m3[d1--d5]	-	-	+	-	-	-	NP
B512m1	+	-	+	-	-	-	our:2004
B512m2	-	+	-	+	-	+	our:2006
B512m2[d1--d2]	-	+	-	+	-	+	our:2006
B512m3	+	-	+	-	-	-	our:2006
B512m3[d1--d3]	+	-	+	-	-	-	our:2006
B513m	-	+	+	+	-	-	our:2006
B513m[d1--d3]	-	+	+	+	-	-	our:2006
B514m	-	+	+	+	+	-	Bonciani, Mastrolia, Remiddi:2002
B514md	-	+	+	+	+	-	our:2004

an example of the set of six
MIs

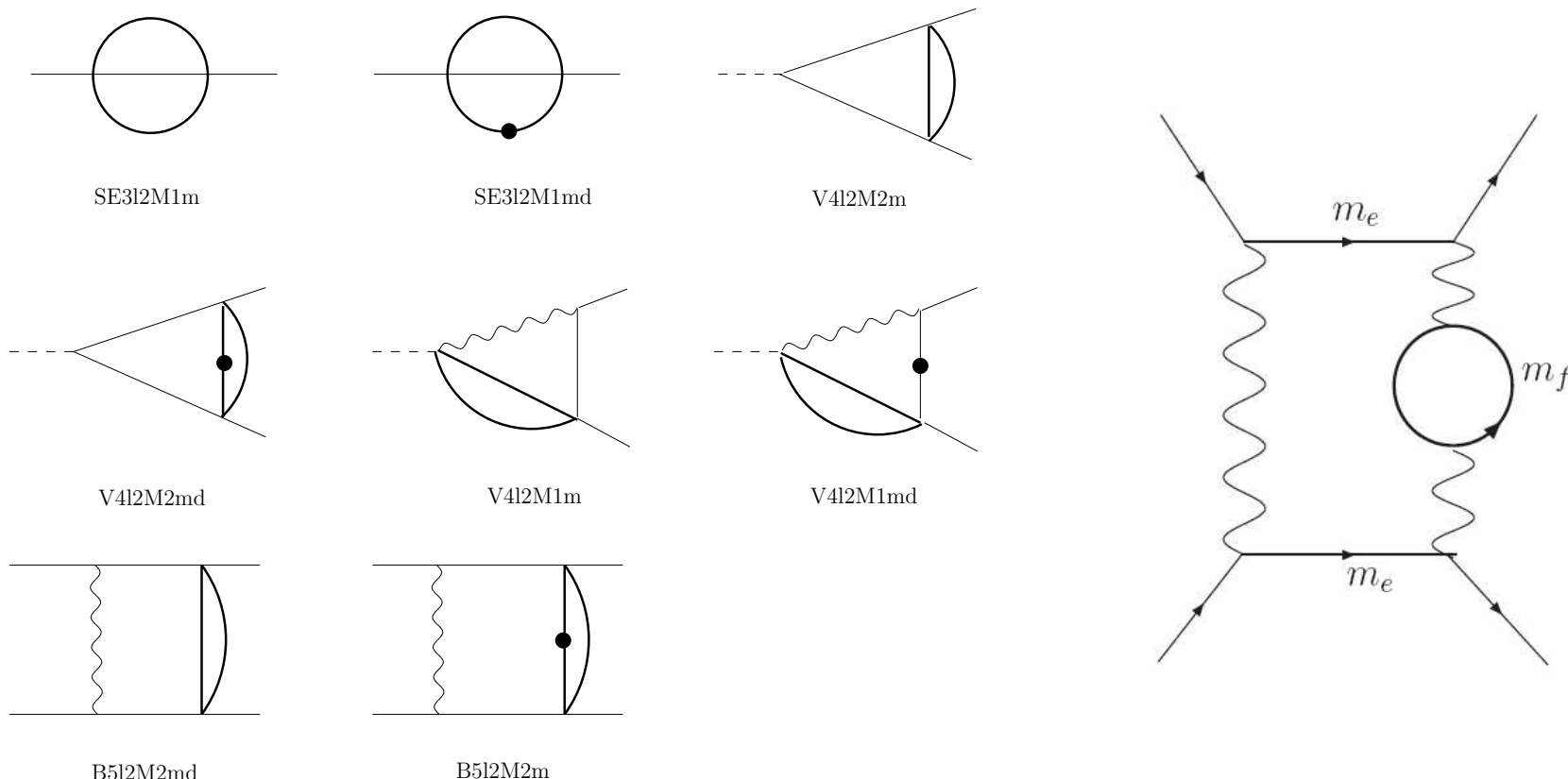


subset of the nonplanar:



The master integrals for the $N_f = 2$ contributions

S. Actis, M. Czakon, JG, T. Riemann, 2006(publ.) / 2007(box master expansion corrected)



There are eight additional master integrals with two different mass scales.

The 2-box-diagrams represent a three-scale problem: $s/m_e^2, t/m_e^2, M^2/m_e^2$

Self-energy master integrals:

S. Actis, M. Czakon, JG, T. Riemann, NPB(PS) 160 (2006) 91, hep-ph/0609051

$$L(R) = \ln \left(\frac{m_e^2}{M^2} \right)$$

$$\begin{aligned} \text{SE312M1m[on shell]} &= M^2 m^{-4\epsilon} \left\{ R \left[\frac{1}{2\epsilon^2} + \frac{5}{4\epsilon} - \frac{3}{8} + \frac{\zeta_2}{2} + \frac{3}{2} L(R) - \frac{1}{2} L^2(R) \right] \right. \\ &+ R^2 \left[\frac{11}{18} - \frac{1}{3} L(R) \right] + \epsilon \left[R \left(\frac{45}{16} + \frac{5}{4} \zeta_2 - \frac{\zeta_3}{3} - \frac{7}{4} L(R) + L^2(R) \right. \right. \\ &\left. \left. - \frac{1}{2} L^3(R) \right) + R^2 \left(-\frac{3}{4} + \frac{8}{9} L(R) - \frac{1}{2} L^2(R) \right) \right], \end{aligned}$$

$$\begin{aligned} \text{SE312M1md[on shell]} &= m^{-4\epsilon} \left\{ \frac{1}{2\epsilon^2} + \frac{1}{2\epsilon} \left[1 + 2L(R) \right] + \frac{1}{2} (1 + \zeta_2) + L(R) + L^2(R) \right. \\ &+ \epsilon \left[\frac{1}{6} (3 + 3\zeta_2 - 2\zeta_3) + (1 + \zeta_2) L(R) + L^2(R) + \frac{2}{3} L^3(R) \right] \\ &+ R \left[-\frac{3}{4} + \frac{1}{2} L(R) + \epsilon \left(\frac{7}{8} - L(R) + \frac{3}{4} L^2(R) \right) \right] \\ &+ R^2 \left[-\frac{5}{36} + \frac{1}{6} L(R) + \epsilon \left(-\frac{5}{72} + \frac{1}{18} L(R) + \frac{1}{4} L^2(R) \right) \right] \left. \right\}. \end{aligned}$$

Vertex master integrals:

Actis,Czakon,JG,Riemann, NPB(PS) 160 (2006) 91, hep-ph/0609051

$L_m(x) = \ln(-m^2/x)$ and $L_M(x) = \ln(-M^2/x)$,

$$\begin{aligned} V412M1m[x] &= m^{-4\epsilon} \left\{ \frac{1}{2\epsilon^2} + \frac{5}{2\epsilon} + \frac{1}{2} \left[19 - 3\zeta_2 - L_m^2(x) \right] \right. \\ &+ \frac{M^2}{x} \left[-2 + 4\zeta_2 - 4\zeta_3 - 2L_m(x) + 2L_M(x) - 4\zeta_2 L_M(x) \right. \\ &\left. \left. + 2L_m(x)L_M(x) - L_M^2(x) - L_m(x)L_M^2(x) + \frac{1}{3}L_M^3(x) \right] \right\}, \end{aligned}$$

$$\begin{aligned} V412M1md[x] &= \frac{m^{-4\epsilon}}{m^2} \left\{ \frac{1}{2\epsilon^2} + \frac{1}{\epsilon} \left[1 + \frac{1}{2}L_m(x) \right] + 2 - \zeta_2 + L_m(x) + \frac{1}{4}L_m^2(x) \right. \\ &+ \frac{M^2}{x} \left[\frac{1}{\epsilon} - \frac{1}{\epsilon}L_M(x) - 1 + 3\zeta_2 + L_m(x) + L_M(x) \right. \\ &\left. \left. - L_m(x)L_M(x) - \frac{1}{2}L_M^2(x) \right] \right\}, \end{aligned}$$

$$V412M2m[x] = m^{-4\epsilon} \left\{ \frac{1}{2\epsilon^2} + \frac{1}{\epsilon} \left[\frac{5}{2} + L_m(x) \right] + \frac{1}{2}(19 + \zeta_2) + 5 L_m(x) + L_m^2(x) \right\},$$

$$V412M2md[x] = \frac{m^{-4\epsilon}}{6x} \left[12\zeta_3 - 6\zeta_2 L_M(x) - L_M^3(x) \right],$$

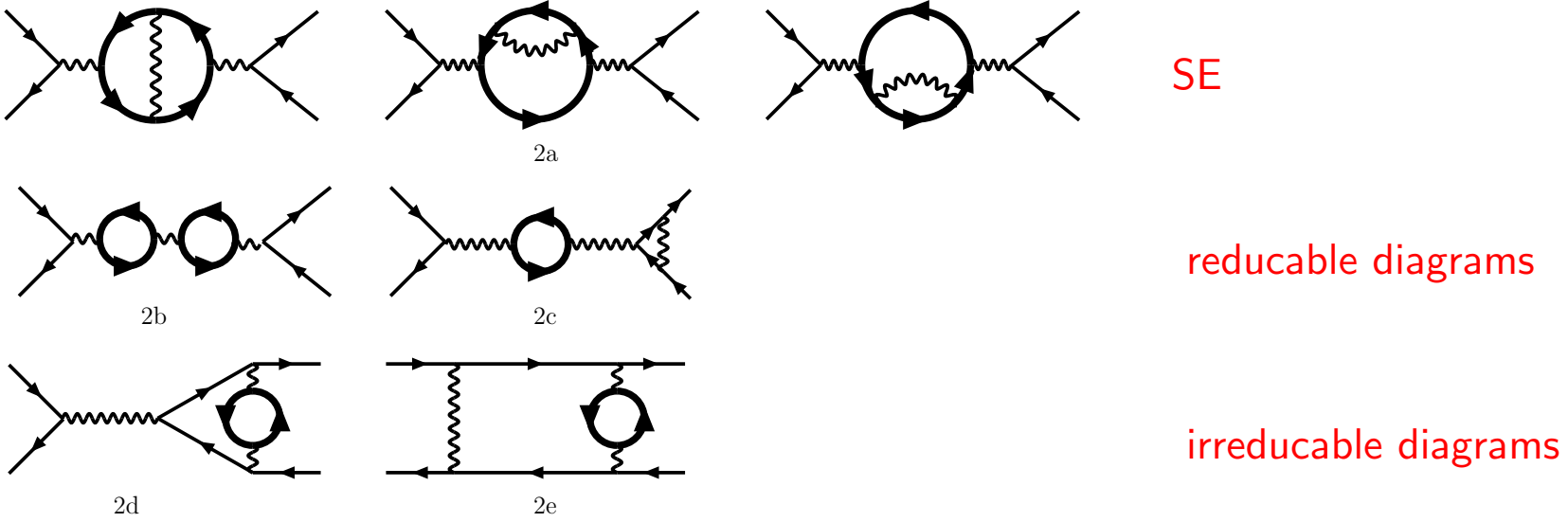
Box master integrals:

Correct Mellin-Barnes representations in Actis et al., NPB(PS) 160 (2006) 91, hep-ph/0609051

But wrong mass expansion there! Correct results are:

$$\begin{aligned} \text{B512M2m}[x, y] = & \frac{m^{-4\epsilon}}{x} \left\{ \frac{1}{\epsilon^2} L_m(x) + \frac{1}{\epsilon} \left(-\zeta_2 + 2L_m(x) + \frac{1}{2} L_m^2(x) + L_m(x)L_m(y) \right) \right. \\ & - 2\zeta_2 - 2\zeta_3 + 4L_m(x) + L_m^2(x) + \frac{1}{3} \textcolor{red}{L_m^3(x)} - 4\zeta_2 L_m(y) \\ & + 2L_m(x)L_m(y) + \textcolor{red}{L_m(x)L_m^2(y)} - \frac{1}{6} \textcolor{red}{L_m^3(y)} \\ & - \left(3\zeta_2 + \frac{1}{2} L_m^2(x) - L_m(x)L_m(y) + \frac{1}{2} L_m^2(y) \right) \ln \left(1 + \frac{y}{x} \right) \\ & \left. - \left(L_m(x) - L_m(y) \right) \text{Li}_2 \left(-\frac{y}{x} \right) + \text{Li}_3 \left(-\frac{y}{x} \right) \right\}, \end{aligned}$$

$$\begin{aligned} \text{B512M2md}[x, y] = & \frac{m^{-4\epsilon}}{xy} \left\{ \frac{1}{\epsilon} \left[-L_m(x)L_m(y) + L_m(x)L(R) \right] - 2\zeta_3 + \zeta_2 L_m(x) + 4\zeta_2 L_m(y) \right. \\ & - 2\textcolor{red}{L_m(x)L_m^2(y)} + \frac{1}{6} \textcolor{red}{L_m^3(y)} - 2\zeta_2 L(R) + 2L_m(x)L_m(y)L(R) - \frac{1}{6} L^3(R) \\ & + \left(3\zeta_2 + \frac{1}{2} L_m^2(x) - L_m(x)L_m(y) + \frac{1}{2} L_m^2(y) \right) \ln \left(1 + \frac{y}{x} \right) \\ & \left. + \left(L_m(x) - L_m(y) \right) \text{Li}_2 \left(-\frac{y}{x} \right) - \text{Li}_3 \left(-\frac{y}{x} \right) \right\}. \end{aligned}$$



Classes of Bhabha-scattering [-loop diagrams](#) containing at least one fermion loop.

After combining the [2-loop](#) terms with the [loop-by-loop](#) terms and with [soft real](#) corrections:

$$\begin{aligned}
 \frac{d\sigma^{\text{NNLO}}}{d\Omega} + \frac{d\sigma_{\gamma}^{\text{NLO}}}{d\Omega} &= \frac{d\sigma^{\text{NNLO},e}}{d\Omega} + \sum_{f \neq e} Q_f^2 \frac{d\sigma^{\text{NNLO,f}^2}}{d\Omega} + \sum_{f \neq e} Q_f^4 \frac{d\sigma^{\text{NNLO,f}^4}}{d\Omega} \\
 &\quad + \sum_{f_1, f_2 \neq e} Q_{f_1}^2 Q_{f_2}^2 \frac{d\sigma^{\text{NNLO,2f}}}{d\Omega}.
 \end{aligned}$$

One of terms:

$$\frac{d\sigma^{\text{NNLO,f}^2}}{d\Omega} = \frac{\alpha^2}{s} \left\{ \sigma_1^{\text{NNLO,f}^2} + \sigma_2^{\text{NNLO,f}^2} \ln \left(\frac{2\omega}{\sqrt{s}} \right) \right\}$$

The $\sigma_1^{\text{NNLO,f}^2}$ (which means box) is the main result of this study

$$\begin{aligned}
\sigma_1^{\text{NNLO,f}^2} = & \frac{(1-x+x^2)^2}{3x^2} \left\{ -\frac{1}{3} \left[\ln^3 \left(\frac{s}{m_e^2} \right) + \ln^3(R_f) \right] + \ln^2 \left(\frac{s}{m_e^2} \right) \left[\frac{55}{6} - \ln(R_f) \right. \right. \\
& + \left. \ln(1-x) - \ln(x) \right] + \ln \left(\frac{s}{m_e^2} \right) \left[-\frac{589}{18} + \frac{37}{3} \ln(R_f) - \ln^2(R_f) \right. \\
& - 2 \ln(R_f) \left(\ln(x) - \ln(1-x) \right) - 8 \text{Li}_2(x) \left. \right] + \frac{4795}{108} - \frac{409}{18} \ln(R_f) + \frac{19}{6} \ln^2(R_f) \\
& - \ln^2(R_f) \left(\ln(x) - \ln(1-x) \right) - 8 \ln(R_f) \text{Li}_2(x) + \frac{40}{3} \text{Li}_2(x) \left. \right\} \\
& + \ln \left(\frac{s}{m_e^2} \right) \left[\zeta_2 \left(-\frac{2}{3x^2} + \frac{4}{3x} + \frac{11}{2} - \frac{23}{3}x + \frac{16}{3}x^2 \right) + \ln^2(x) \left(-\frac{1}{3x^2} + \frac{17}{12x} \right. \right. \\
& - \frac{5}{4} - \frac{x}{12} + \frac{2}{3}x^2 \left. \right) + \ln^2(1-x) \left(-\frac{2}{3x^2} + \frac{11}{6x} - \frac{5}{2} + \frac{11}{6}x - \frac{2}{3}x^2 \right) \\
& + \ln(x) \ln(1-x) \left(\frac{2}{3x^2} - \frac{4}{3x} - \frac{1}{2} + \frac{5}{3}x - \frac{4}{3}x^2 \right) + \ln(x) \left(\frac{55}{9x^2} - \frac{83}{9x} + \frac{65}{6} \right. \\
& - \frac{85}{18}x + \frac{10}{9}x^2 \left. \right) + \frac{1}{3} \ln(1-x) \left(-\frac{10}{3x^2} + \frac{31}{6x} - 10 + \frac{31}{6}x - \frac{10}{3}x^2 \right) \left. \right] \\
& + \frac{1}{3} \ln^3(x) \left(-\frac{1}{3x^2} + \frac{31}{12x} - \frac{11}{6} - \frac{x}{6} + \frac{x^2}{3} \right) + \frac{1}{3} \ln^3(1-x) \left(-\frac{1}{3x^2} + \frac{1}{x} \right. \\
& - \frac{4}{3} + x - \frac{x^2}{3} \left. \right) + \ln^2(x) \ln(1-x) \left(-\frac{1}{3x^2} + \frac{1}{3x} - \frac{4}{3} + x - \frac{x^2}{3} \right) \\
& + \frac{1}{3} \ln(x) \ln^2(1-x) \left(-\frac{1}{x^2} + \frac{2}{x} - \frac{7}{4} + \frac{x}{2} \right) + \ln^2(x) \left[\frac{55}{18x^2} - \frac{46}{9x} + \dots \right]
\end{aligned}$$

$$\begin{aligned}
& \dots + \frac{14}{3} - \frac{4}{9}x - \frac{10}{9}x^2 + \ln(R_f) \left(-\frac{1}{3x^2} + \frac{17}{12x} - \frac{5}{4} - \frac{x}{12} + \frac{2}{3}x^2 \right) \\
& + \ln^2(1-x) \left[\frac{10}{9x^2} - \frac{29}{9x} + \frac{9}{2} - \frac{29}{9}x + \frac{10}{9}x^2 + \ln(R_f) \left(-\frac{2}{3x^2} + \frac{11}{6x} \right. \right. \\
& \left. \left. - \frac{5}{2} + \frac{11}{6}x - \frac{2}{3}x^2 \right) \right] + \ln(x) \ln(1-x) \left[-\frac{10}{9x^2} + \frac{37}{18x} + \frac{1}{2} - \frac{25}{9}x \right. \\
& \left. + \frac{20}{9}x^2 + \ln(R_f) \left(\frac{2}{3x^2} - \frac{4}{3x} - \frac{1}{2} + \frac{5}{3}x - \frac{4}{3}x^2 \right) \right] + \ln(x) \left[-\frac{589}{54x^2} + \frac{1753}{108x} \right. \\
& \left. - \frac{701}{36} + \frac{925}{108}x - \frac{56}{27}x^2 + \text{Li}_2(x) \left(-\frac{4}{x^2} + \frac{19}{3x} - 7 + 3x - \frac{2}{3}x^2 \right) \right. \\
& \left. + \ln(R_f) \left(\frac{37}{9x^2} - \frac{56}{9x} + \frac{47}{6} - \frac{67}{18}x + \frac{10}{9}x^2 \right) + \zeta_2 \left(-\frac{2}{3x^2} + \frac{4}{x} - \frac{1}{6} \right. \right. \\
& \left. \left. - \frac{10}{3}x + 2x^2 \right) \right] + \ln(1-x) \left[\frac{56}{27x^2} - \frac{161}{54x} + \frac{56}{9} - \frac{161}{54}x + \frac{56}{27}x^2 \right. \\
& \left. + \ln(R_f) \left(-\frac{10}{9x^2} + \frac{31}{18x} - \frac{10}{3} + \frac{31}{18}x - \frac{10}{9}x^2 \right) + \zeta_2 \left(-\frac{2}{x^2} + \frac{20}{3x} - \frac{32}{3} + \frac{20}{3}x \right. \right. \\
& \left. \left. - 2x^2 \right) \right] + \text{Li}_3(x) \left(\frac{4}{3x^2} - \frac{7}{3x} + 3 - \frac{5}{3}x + \frac{2}{3}x^2 \right) + \frac{2}{3}S_{1,2}(x) \left(-\frac{1}{x^2} + \frac{1}{x} \right. \\
& \left. - x + x^2 \right) + \zeta_2 \left[\frac{19}{9x^2} - \frac{13}{18x} - \frac{43}{3} + \frac{311}{18}x - \frac{98}{9}x^2 + \ln(R_f) \left(-\frac{2}{3x^2} + \frac{4}{3x} \right. \right. \\
& \left. \left. + \frac{11}{2} - \frac{23}{3}x + \frac{16}{3}x^2 \right) \right] + \zeta_3 \left(-\frac{4}{3x^2} + \frac{3}{x} - 5 + \frac{11}{3}x - 2x^2 \right)
\end{aligned}$$

Small angle, $\Theta = 3^\circ$, $m_e^2 \ll m_f^2 \ll s, t, u$

$d\sigma / d\Omega$ [nb] \sqrt{s} [GeV]	10	91	500
LO QED	440873	5323.91	176.349
LO Zfitter	440875	5331.5	176.283
NNLO (e)	-1397.35	-35.8374	-1.88151
NNLO ($e + \mu$) our	-1394.74	-43.1888	-2.41643
NNLO ($e + \mu + \tau$) our			-2.55179
NNLO photonic	9564.09	251.661	12.7943

Table 2: Numerical values for the NNLO corrections to the differential cross section respect to the solid angle. Results are expressed in nanobarns for a scattering angle $\theta = 3^\circ$. Empty entries are related to cases where the high-energy approximation cannot be applied.

Large angle, with $\Theta = 90^\circ$, $m_e^2 \ll m_f^2 \ll s, t, u$

$d\sigma / d\Omega$ [nb] \sqrt{s} [GeV]	10	91	500
LO QED	0.466409	0.00563228	0.000186564
LO Zfitter	0.468499	0.127292	0.0000854731
NNLO (e)	-0.00453987	-0.0000919387	-4.28105 · 10⁻⁶
NNLO ($e + \mu$) our	-0.00570942	-0.000122796	-5.90469 · 10⁻⁶
NNLO ($e + \mu + \tau$) our	-0.00586082	-0.000135449	-6.7059 · 10⁻⁶
NNLO ($e + \mu + \tau + t$) our			-6.6927 · 10⁻⁶
NNLO photonic	0.0358755	0.000655126	0.0000284063

Table 3: Numerical values for the NNLO corrections to the differential cross section respect to the solid angle. Results are expressed in nanobarns for a scattering angle $\theta = 90^\circ$. Empty entries are related to cases where the high-energy approximation cannot be applied.

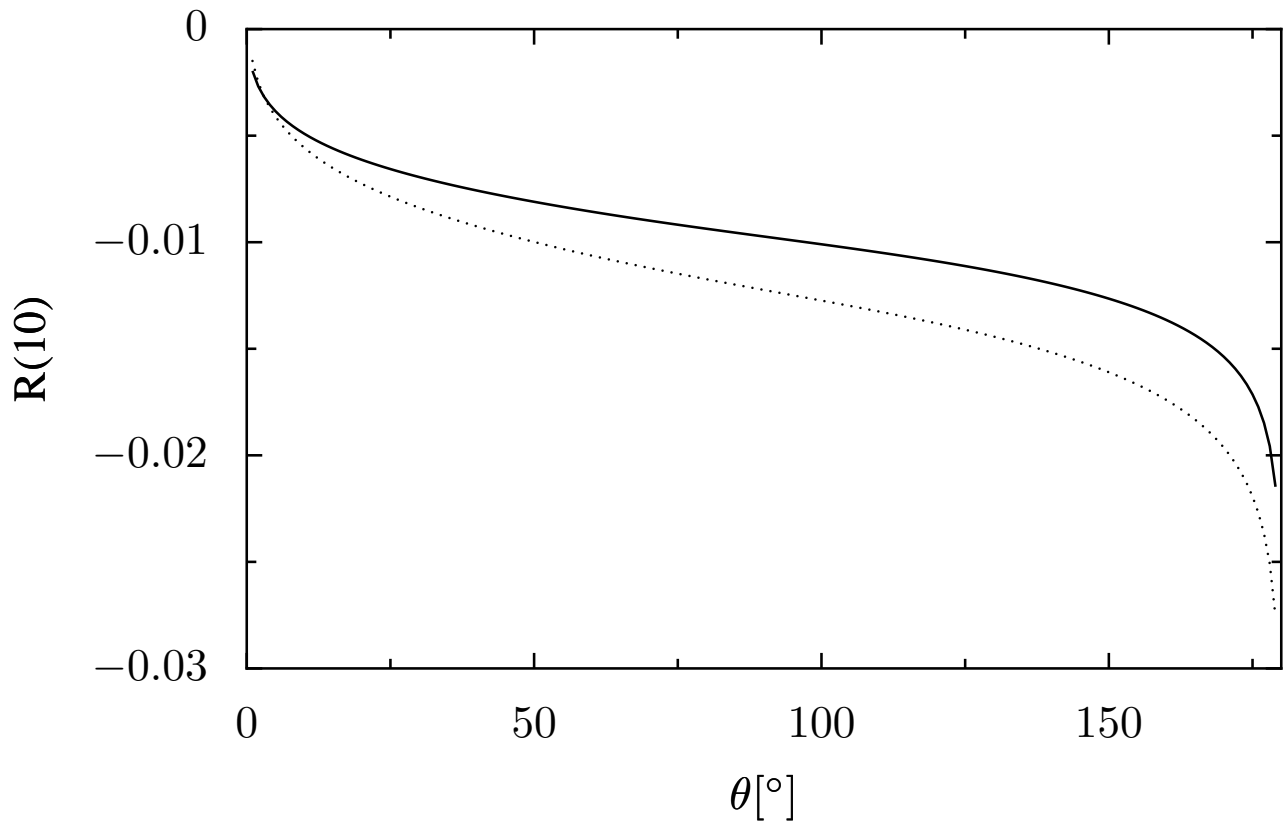


Figure 1: Ratio of the fermionic NNLO corrections to the differential cross section respect to the tree-level result for $\sqrt{s} = 10$ GeV. **Solid** line: electron-loop contributions, a **dotted** one the sum of electron- and muon-loop ones, and a **dashed** one includes also τ leptons.

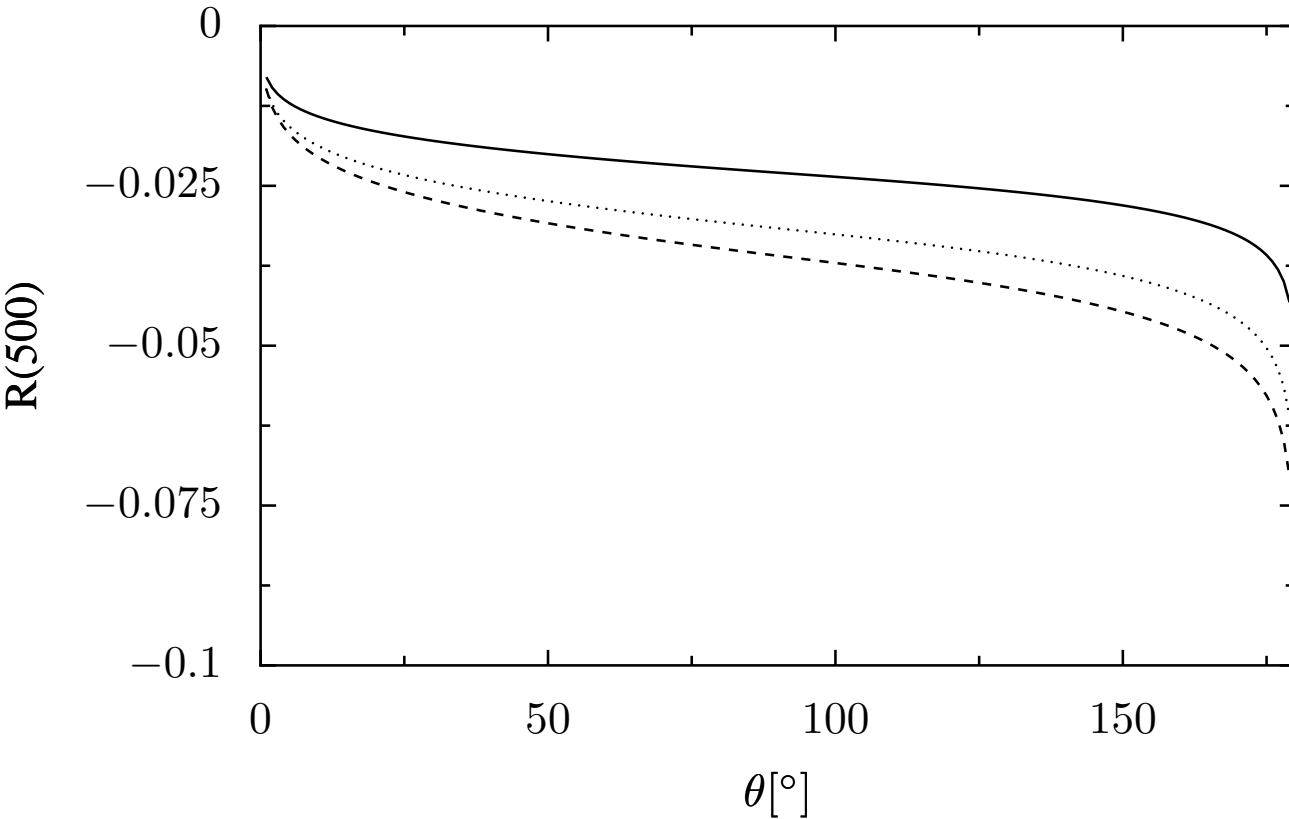


Figure 2: Ratio of the fermionic NNLO corrections to the differential cross section respect to the tree-level result for $\sqrt{s} = 500$ GeV. **Solid** line: electron-loop contributions, a **dotted** one the sum of electron- and muon-loop ones, and a **dashed** one includes also τ leptons.

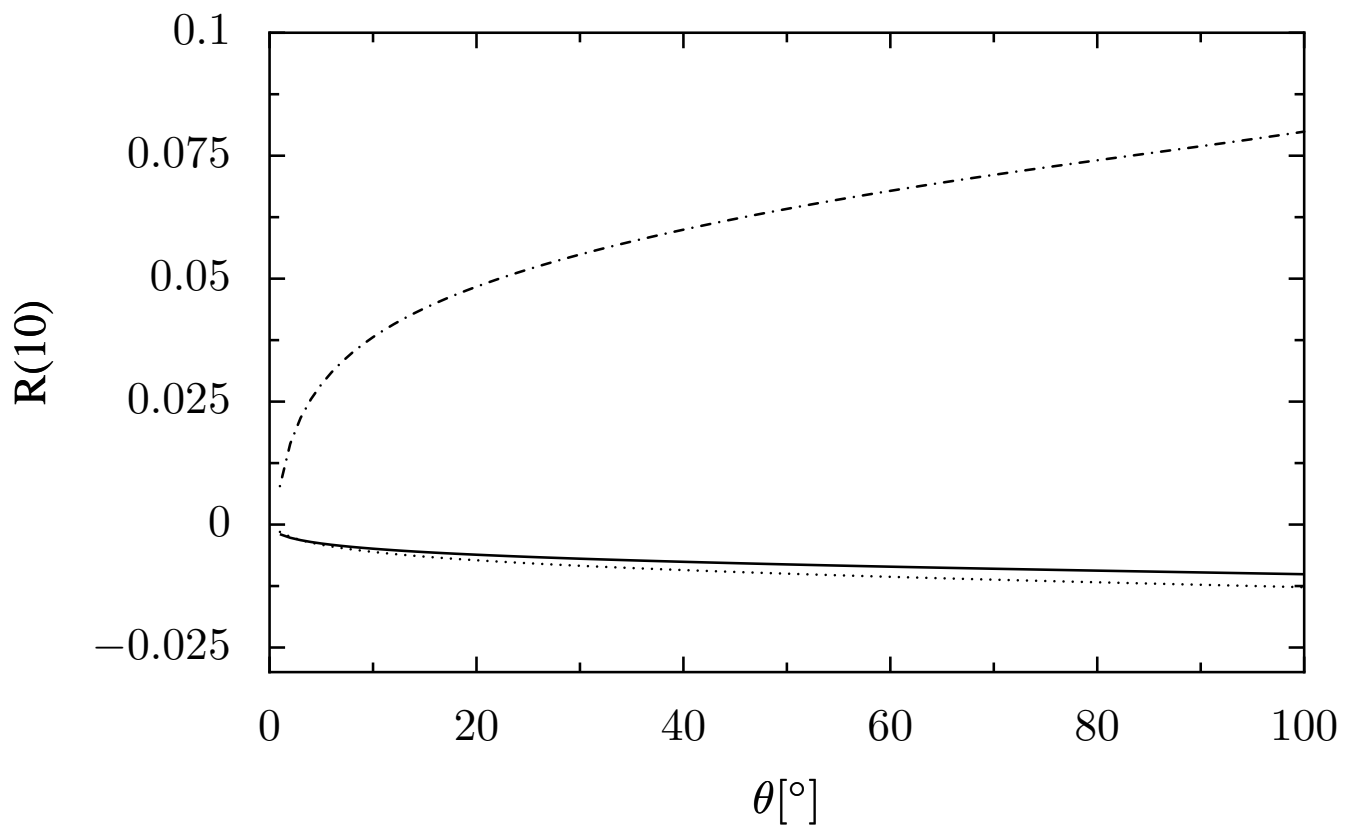


Figure 3: Here also with the photonic (opposite sign) contributions (dash-dotted lines).

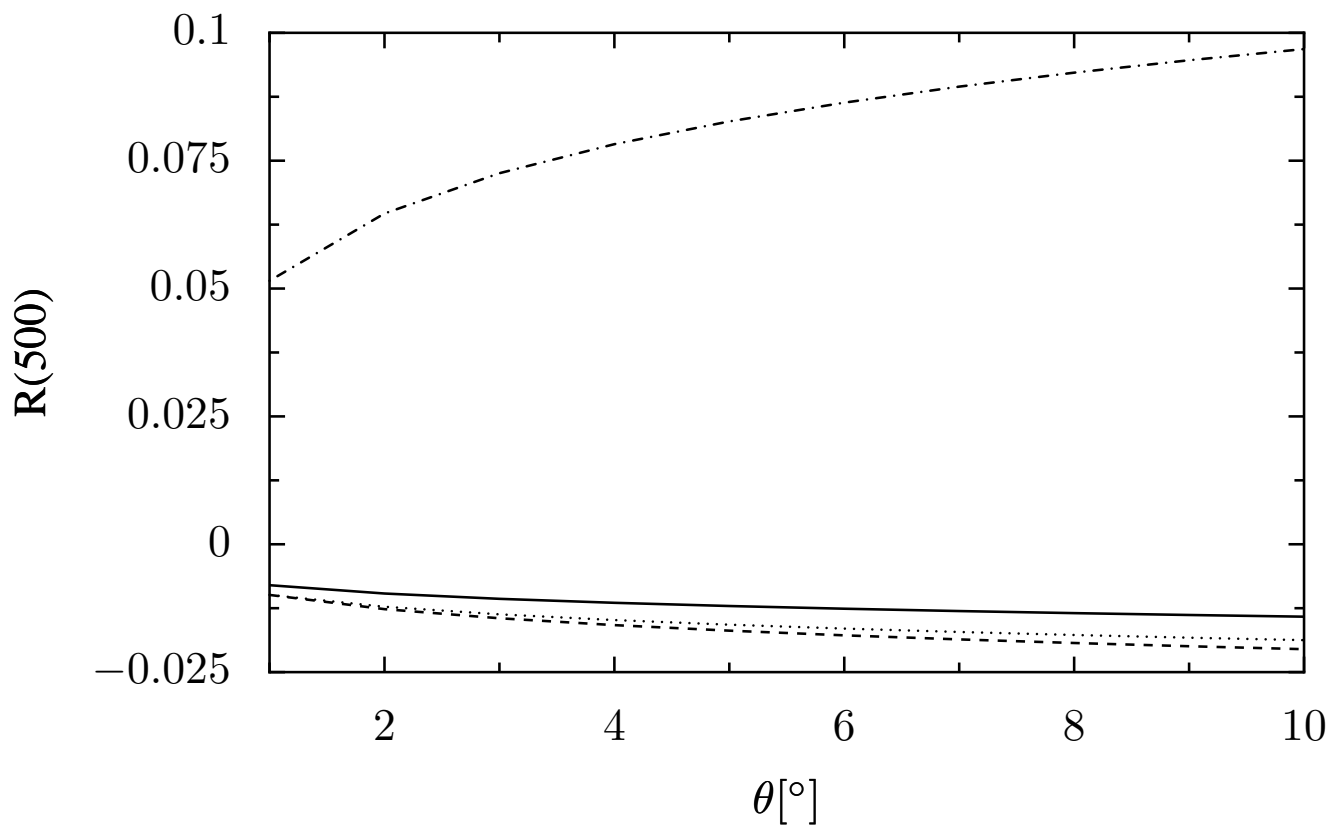


Figure 4: Here also with the photonic (opposite sign) contributions (dash-dotted lines).

Summary I

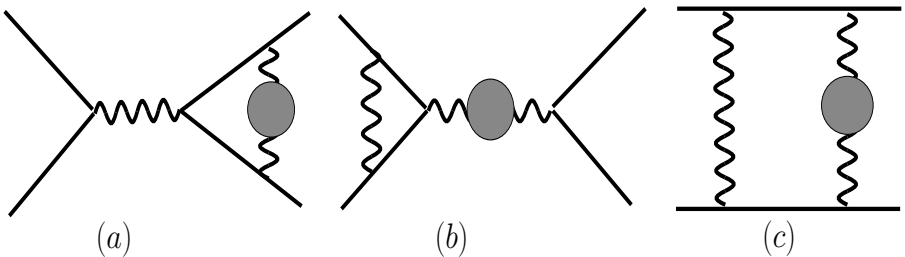
- We determined the $N_f = 2$ contributions to 2-loop Bhabha scattering
- The contribution is small, but non-negligible at the scale 10^{-4}
There is no decoupling of the heavier fermions (as indeed there shouldn't, since the typical scale of the process is large compared to all the masses), the electron loop contributions dominate in the fermionic part.
- Agreement with:
"Two-loop QED corrections to Bhabha scattering"
Thomas Becher (Fermilab) , Kirill Melnikov (Hawaii U.), arXiv:0704.3582 [hep-ph],
subm. to JHEP

but, as $m_f^2 \ll s, t, u$, so far

- no top quark
- no calculations for meson factories (down to 1 GeV)
- no hadronic corrections (light quarks, nonperturbative effects)

all these drawbacks can be removed by usage dispersion integrals

Three classes of two-loop hadronic/fermionic Bhabha diagrams



Propagator

$$\frac{g_{\mu\nu}}{q^2 + i\delta} \rightarrow \frac{g_{\mu\alpha}}{q^2 + i\delta} (q^2 g^{\alpha\beta} - q^\alpha q^\beta) \Pi_{\text{had}}(q^2) \frac{g_{\beta\nu}}{q^2 + i\delta}$$

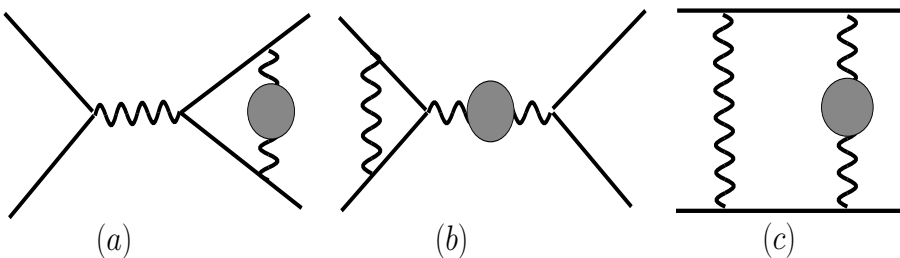
and fermion loop insertion replaced by the dispersion integral

$$\Pi_{\text{had}}(q^2) = -\frac{q^2}{\pi} \int_{4M_\pi^2}^{\infty} \frac{dz}{z} \frac{\text{Im} \Pi_{\text{had}}(z)}{q^2 - z + i\delta}$$

Finally $\text{Im} \Pi_{\text{had}}(z)$ can be related to the experimental data

$$\text{Im} \Pi_{\text{had}}(z) = -\frac{\alpha}{3} R_{\text{had}}(z), \quad R_{\text{had}}(z) = -\frac{\alpha}{3} \frac{\sigma_{e^+ e^- \rightarrow \text{hadrons}}(z)}{(4\pi\alpha^2)/(3z)}.$$

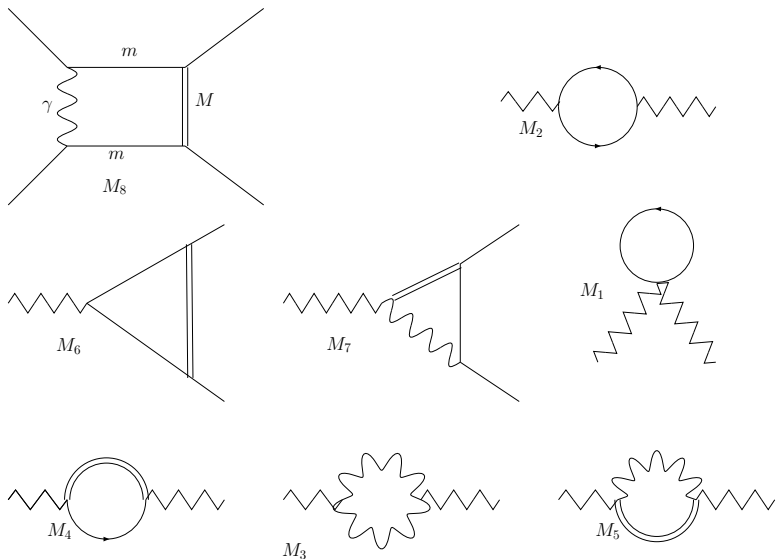
In the context of Bhabha process



- Dispersion method used for (one-loop) propagator insertions (Cabibbo, Gato, 1961)
- applied to two-loop irreducible vertex (Kniehl, Krawczyk, Kühn, Stuart, 1988)

now we complete with boxes

Masters



Mass M is an integrable variable z

Box can be written through the convolution of a kernel function K with the hadronic cross-section ratio R_{had} ,

$$B_{had}(s, t) = \int_{4M_\pi^2}^\infty \frac{dz}{z} R_{had}(z) K(s, t, z).$$

For leptons and the top quark, we have to replace $4M_\pi^2 \rightarrow 4m_f^2$ and $R_{had} \rightarrow R_{fer}$, given by

$$R_{fer}(z) = Q_f^2 C_f \sqrt{1 - 4 \frac{m_f^2}{z}} \left(1 + 2 \frac{m_f^2}{z} \right)$$

Kernels

The three box kernels have been derived with the aid of the master integrals in the limit $m_e^2 \ll m_f^2, s, t$. The master integrals were determined with IdSolver and evaluated with the Mathematica packages ambre (Mellin-Barnes representations) and eventually mass expanded with a Mathematica package. Numerical cross checks have been made with MB package.

The result for one of kernels:

$$\begin{aligned} K_C(x, y, z) = & \frac{1}{3m_e^2(y-z)} \left\{ 2 \frac{F_\epsilon}{\epsilon} x^2 L_x + 4 \zeta_2 x^2 \left(\frac{z}{y} - 2 \right) - 2(x^2 + y^2 \right. \\ & + xy) L_x + x^2 \left(\frac{z}{y} - 1 \right) L_y + 2x^2 \left(\frac{z}{y} - 1 \right) L_y^2 + 4x^2 L_x L_y \\ & + x^2 \left(\frac{z}{y} - 1 \right) \ln \left(\frac{z}{m_e^2} \right) - 2x^2 \left(\frac{z}{y} - \frac{1}{2} \right) \ln^2 \left(\frac{z}{m_e^2} \right) + 4x^2 \left(\frac{z}{y} \right. \\ & - 1) \ln \left(\frac{z}{m_e^2} \right) \ln \left(1 - \frac{z}{y} \right) + 2x^2 \ln \left(\frac{z}{m_e^2} \right) L_x - x^2 \left(\frac{z}{y} + \frac{y}{z} \right. \\ & - 2) \ln \left(1 - \frac{z}{y} \right) - 4x^2 \ln \left(1 - \frac{z}{y} \right) L_x + 4x^2 \left(\frac{z}{y} - 1 \right) \text{Li}_2 \left(\frac{z}{y} \right) \\ & \left. - 2x^2 \text{Li}_2 \left(1 + \frac{z}{x} \right) \right\}, \end{aligned}$$

it is IR divergent, so we add appropriate diagrams ...

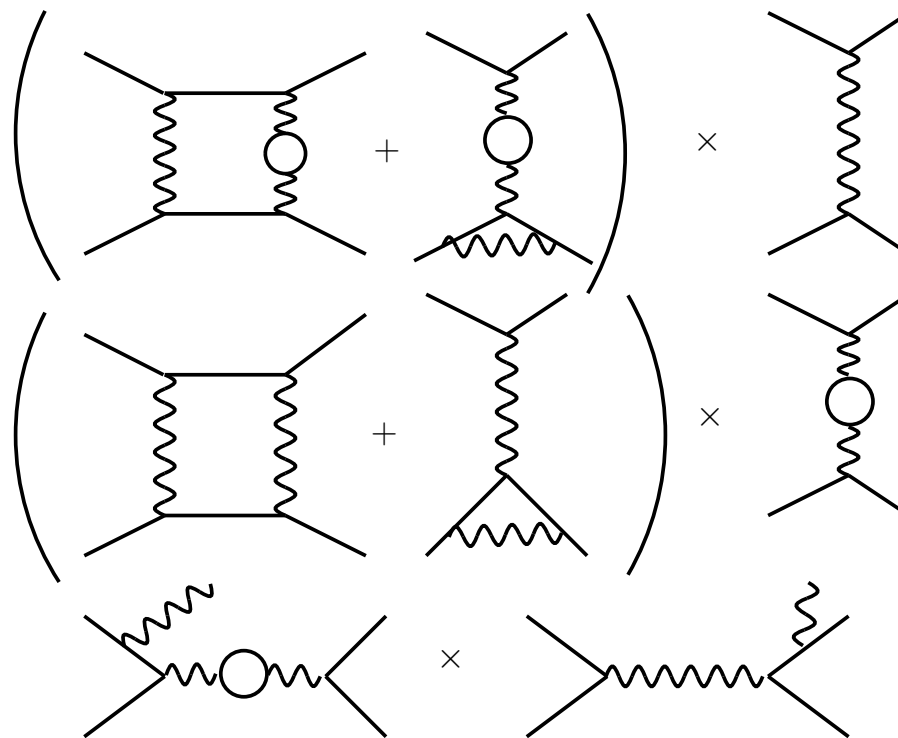


Figure 5: The fermionic two-loop boxes combine with other diagrams to an infrared-finite cross-section contribution.

IR safe boxes

$$\begin{aligned}\frac{d\sigma^{\text{rest}}}{d\Omega} &= \left(\frac{\alpha}{\pi}\right)^2 \frac{\alpha^2}{s} \left\{ \int_{4M^2}^{\infty} dz \frac{R(z)}{z} \frac{1}{t-z} F_1(z) \right. \\ &+ \mathbf{Re} \int_{4M^2}^{\infty} dz \frac{R(z)}{z} \frac{1}{s-z+i\delta} \left[F_2(z) + F_3(z) \ln\left(1 - \frac{z}{s+i\delta}\right) \right] \\ &\left. + \pi \mathbf{Im} \int_{4M^2}^{\infty} dz \frac{R(z)}{z} \frac{1}{s-z+i\delta} F_4(z) \right\}.\end{aligned}$$

e.g. F_1 :

$$\begin{aligned}
F_1(z) = & \frac{1}{3} \left\{ \left[3 \left(\frac{t^2}{s} + 2 \frac{s^2}{t} \right) + 9(s+t) \right] \ln \left(\frac{s}{m_e^2} \right) + \left[-z^2 \left(\frac{1}{s} + \frac{2}{t} + 2 \frac{s}{t^2} \right) \right. \right. \\
& + z \left(4 + 4 \frac{s}{t} + 2 \frac{t}{s} \right) + \frac{1}{2} \frac{t^2}{s} + 6 \frac{s^2}{t} + 5s + 4t \left. \right] \ln \left(-\frac{t}{s} \right) + s \left(-\frac{z}{t} + \frac{3}{2} \right) \\
& \times \ln \left(1 + \frac{t}{s} \right) \dots \dots \dots \\
& - \left[\frac{z^2}{t} - 2z \left(1 + \frac{s}{t} \right) + \frac{t^2}{s} + 5s + 2 \frac{s^2}{t} + 4t \right] \text{Li}_2 \left(1 + \frac{z}{u} \right) \Big\} \\
& + 4 \left(\frac{1}{3} \frac{t^2}{s} + \frac{2}{3} \frac{s^2}{t} + s + t \right) \ln \left(\frac{2\omega}{\sqrt{s}} \right) \left[\ln \left(\frac{s}{m_e^2} \right) + \ln \left(-\frac{t}{s} \right) \right. \\
& \left. \left. - \ln \left(1 + \frac{t}{s} \right) - 1 \right].
\end{aligned}$$

Results: nice agreement where $m_e^2 \ll m_f^2 \ll s, t, u$ applicable

\sqrt{s} [GeV]	1	10	M_Z	500
QED Born	440994	4409.94	53.0348	1.76398
rest e	193	5.73	0.1357	0.00673
μ	< 1 x	0.42 0.08	0.0408 0.0407	0.00288 0.00288
τ	< 1 x	$< 10^{-2}$ x	0.0027 -0.0096	0.00088 0.00084
t	< 1 x	$< 10^{-2}$ x	$< 10^{-4}$ x	$< 10^{-5}$ x

Table 4: Numerical values for the differential cross section in nanobarns at a scattering angle $\theta = 3^\circ$, in units of 10^2 . Blue entries are obtained with dispersion relations. Red are analytical results in the limit $m_e^2 \ll m_f^2 \ll s, t, u$

\sqrt{s} [GeV]	1	10	M_Z	500
QED Born	466537	4665.37	56.1067	1.86615
full Born	466558	4686.27	1273.2680	0.85496
rest e	807	14.53	0.2706	0.01193
μ	160 153	6.08 6.08	0.1470 0.1470	0.00726 0.00726
τ	2 \times	1.33 1.07	0.0752 0.0752	0.00457 0.00457
t	< 1 \times	$< 10^{-2}$ \times	0.0005 \times	0.00043 -0.00013

Table 5: Numerical values for the differential cross section in nanobarns at a scattering angle $\theta = 90^\circ$, in units of 10^{-4} . Blue entries are obtained with dispersion relations. Red are analytical results in the limit $m_e^2 \ll m_f^2 \ll s, t, u$

Finally: hadrons

To calculate R_{had} , we used rhad.f by H. Burkhardt

small angle

\sqrt{s} [GeV]	1	10	M_Z	500
QED Born	440994	4409.94	53.0348	1.76398
ew. Born	440994	4409.95	53.0370	1.76331
self energies (A)	445291	4495.45	55.5352	1.90910
irred. vertices (B)	-56	-2.74	-0.1005	-0.00704
boxes+red. (C) e	193	5.73	0.1357	0.00673
μ	< 1	0.42	0.0408	0.00288
	—	0.08	0.0407	0.00288
τ	< 1	$< 10^{-2}$	0.0027	0.00088
	—	—	-0.0096	0.00084
t	< 1	$< 10^{-2}$	$< 10^{-4}$	$< 10^{-5}$
	—	—	—	—
had	< 1	0.39	0.0877	0.00811
$\sum_{\text{boxes+red.}}$ (C)	193	6.54	0.2669	0.01254
A + B + C	445428	4501.99	55.8021	1.92164

Table 6: Differential cross sections in nanobarns, in units of 10^2 . A – QED Born + self-energy corrections; B – irreducible vertex corrections, C – net sum of infrared-sensitive corrections

large angle

\sqrt{s} [GeV]	1	10	M_Z	500
QED Born	466537	4665.37	56.1067	1.86615
ew. Born	466558	4686.27	1289.3011	0.85496
self energies (A)	457524	4563.61	57.5091	1.97971
irred. vertices (B)	-494	-14.35	-0.4239	-0.02602
boxes + red. e	807	14.53	0.2706	0.01193
μ	160	6.08	0.1470	0.00726
	153	6.08	0.1470	0.00726
τ	2	1.33	0.0752	0.00457
	—	1.07	0.0752	0.00457
t	< 1	$< 10^{-2}$	0.0005	0.00043
	—	—	—	-0.00013
had.	234	16.07	0.4701	0.02461
$\sum_{\text{boxes+red.}}$ (C)	1203	38.01	0.9634	0.0488
A + B + C	446495	4533.46	56.4986	1.9579

Table 7: The same but for a scattering angle $\theta = 90^\circ$, in units of 10^{-4} .

Summary II

- All two loop virtual QED ($n_f = 1, 2$) corrections to Bhabha scattering are known.
- hadronic corrections are substantial, for example, at small angles at LEP we obtain an additional correction of about 0.16% from the hadronic insertions C, and at large angles at meson factories we get 0.05% to 0.35% from them
- we are going to make more detailed “anatomy” studies of separate contributions (SE, vertices, boxes, log terms, nologs ...)